Global NEST Journal, Vol 26, No 6, 06163

Chlorophyll-enriched chitosan-CuO-ZnO nanoparticles for antimicrobial activities

Muhammad Junaid Khan[1], Saba Saeed[1]*, Umar Draz[2], Muhammad Abid[3], Rabia Ejaz[4], Saltanat Aghayeva[5], Saeedah Musaed Almutairi[6], Najd Talha Bin Talha[6] and Rashid Iqbal[7]*

[1]Institute of Physics, The Islamia University of Bahawalpur, Bahawalpur–63100, Pakistan
[2]Department of Zoology, Emerson University Multan, Pakistan
[3]Department of Mechanical Engineering, COMSATS University Islamabad, Sahiwal Campus
[4]Frontiers Science Center for Rare Isotopes & School of Nuclear Science and Technology, Lanzhou University, Lanzhou 730000, China
[5]Department of Life Sciences, Western Caspian University, Baku, Azerbaijan
[6]Department of Botany and Microbiology, College of Science, King Saud University, P.O. 2455, Riyadh 11451, Saudi Arabia
[7]Department of Agronomy, Faculty of Agriculture and Environment, The Islamia University of Bahawalpur, Bahawalpur 63100, Pakistan
Received: 11/05/2024, Accepted: 23/06/2024, Available online: 26/06/2024
*to whom all correspondence should be addressed: saba.saeed@iub.edu.pk; rashid.iqbal@iub.edu.pk
https://doi.org/10.30955/gnj.006163

Graphical abstract

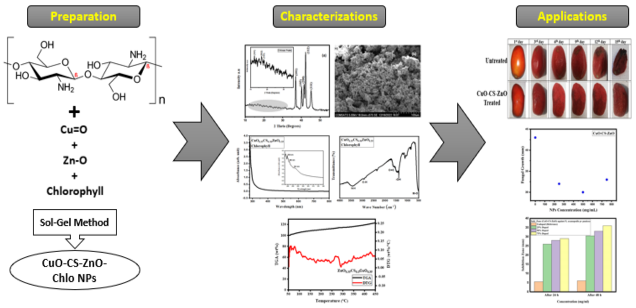

Abstract

Chitosan-doped copper oxide and zinc oxide nanoparticles (CuO-CS-ZnO-Chlo NPs) were prepared utilizing a sol-gel synthesis route. Chlorophyll was added in the process of making NPs to enhance the effects of these NPs. The prepared NPs were thoroughly analyzed using advanced techniques including X-ray diffraction (XRD), scanning electron microscopy (SEM), UV-visible (UV-Vis) spectroscopy, Fourier-transform infrared (FTIR) spectroscopy, and thermogravimetric analysis (TGA). Structural analysis revealed the successful synthesis of irregularly shaped NPs with an average crystallite size of 10.7 nm. In optical properties, UV-Vis showed the absorption bands associated with different absorption centers in the sample and FTIR revealed various function groups associated with the preparation procedure and chemical used while synthesizing these NPs. On the application side, these NPs efficiently resist the growth of *X. axanopodis pv punicea* bacteria within 24-48 hours of investigation. The same NPs showed effective antifungal effects on the Alternaria *solani*. Finally, these NPs were used as food preservative agents whereas tomatoes were used as the target fruit. Tomatoes coated with NPs exhibited better preservation and a longer shelf life.

Keywords: Chitosan, chlorophyll, nanoparticles, antibacterial, antifungal, food preservation

1. Introduction

Nanotechnology unlocks new capabilities by utilizing the qualities of materials at a very small scale through the use of NPs (Ahila *et al.*; Benettayeb *et al.* 2023). It has been shown that nanomaterials can damage important components found within bacterial cells, therefore using nano-metal particles to fight germs can be an effective approach (Hermanto *et al.* 2024; Murtaza, Ahmed, *et al.* 2024; Said *et al.* 2024; Salas-Orozco *et al.* 2024). Nanoscale particles come in a variety of shapes and sizes, including atomic clusters, nanorods, dots, grains, fibers, films, and nanopores, all with large surface areas. These materials have better physicochemical properties than regular alternatives. They have been extensively explored and show promising antibacterial, antiviral, and antifungal effects (Nizami *et al.* 2021). Furthermore, NPs are known for their antibacterial characteristics, which inhibit the growth of microorganisms. This has resulted in its extensive use in dentistry. NPs are used in many dentistry sectors because of their potential to prevent infections and promote oral health (Dizaj 2015; Khurshid *et al.* 2015; Murtaza *et al.* 2024; Parnia *et al.* 2017). NPs, having distinct features, are used in the food industry for preservation. Their antibacterial activity, mediated by processes such as oxygen species and membrane disruption, improves food safety. Nanotechnology-based packaging provides a better barrier, mechanical strength, and biodegradability for longer food preservation (Ghosh *et al.* 2019). NPs offer intriguing possibilities for treating fungal infections by increasing medicine delivery. They improve medication properties, such as pharmacodynamics, resulting in lower toxicity and extended effects. Nanotechnology promises novel methods for antifungal treatment and larger uses in infectious disorders (Renzi *et al.* 2021). Metal oxide NPs have strong antibacterial properties without affecting surrounding tissues, making them useful in textiles, water treatment, medicine, and food packaging. Their use reduces the toxicity concerns associated with organic disinfectants (Hajipour *et al.* 2012; Naseem and Durrani 2021; Singh *et al.* 2008; Tang and Zheng 2018).

CS, a versatile biopolymer, is made from chitin, a structural component present in the exoskeletons of crustaceans such as shrimp and crab. Chitin is transformed into CS via a process known as deacetylation, which alters its chemical structure and increases its solubility and usefulness. Due to its qualities, it is useful for tissue engineering, medication delivery, and wound healing, all of which hold promise for improvements in industrial and medical applications (Kou *et al.* 2021; Wu *et al.* 2023; T. Zhang *et al.* 2023). CS NPs, made from CS, are nanoscale particles with numerous applications. With improved qualities such as biocompatibility and specific distribution, they show potential in various industries, including medicine and agriculture (Fan *et al.* 2024; Fonseca *et al.* 2024; Jalal *et al.* 2023). The strong antibacterial qualities of CS NPs make them useful in the fight against infections and the creation of new antimicrobial agents for a range of applications (Benettayeb *et al.* 2023; Jha and Mayanovic 2023; Poznanski *et al.* 2023).

Similarly, Ag, Cu, CuO, and ZnO are examples of metallic materials that have been utilized to create antibacterial materials. Bacteria and viruses cell membranes are susceptible to the release of cations and reactive oxygen species caused by metallic materials. ZnO and CuO are two of the most commonly utilized metallic oxides because they are inexpensive, simple to produce, and have antibacterial qualities that make them useful in biological applications (Abdelrazek *et al.* 2023; Alturki 2022; Bolaina-Lorenzo *et al.* 2022; Boshkova *et al.* 2023; Govindasamy *et al.* 2023; Matyjasik *et al.* 2022). ZnO NPs improve food packaging films made of biopolymers by providing better fresh food preservation and minimizing zinc migration, which complies with safety standards (Chen *et al.* 2024; Espitia *et al.* 2012; Kim *et al.* 2022; Zare *et al.* 2022; W. Zhang *et al.* 2023). Fruit shelf life is extended when CuO NPs are incorporated into CS and hydroxypropyl cellulose-based bio-nanocomposites. This emphasizes the potential of these materials for active food packaging (Gunaki *et al.* 2024; Nemr *et al.* 2024; Saleem *et al.* 2024; Shankar *et al.* 2024). Orange juice shelf life is increased with polylactic acid sheets coated with polyaniline, ZnO, and CuO, which improves their antioxidant and antibacterial properties (Abdolsattari *et al.* 2022; Neethidevan *et al.* 2023; Serouti *et al.* 2024). Utilizing the qualities of CS and a variety of metal oxides, CS metal oxide NPs provide environmentally friendly methods of pollution removal for environmental remediation applications (Almaieli *et al.* 2022; Baroudi *et al.* 2023; Jiang *et al.* 2023; Rajivgandhi *et al.* 2023). CS-ZnO NPs provide a strong defense against microbiological challenges in applications related to food safety, healthcare, and sanitation by combining the antibacterial qualities of CS with the enhanced activity of ZnO (Ibrahim *et al.* 2024; Salama and Aziz 2023). With their strong antibacterial, antibiofilm, antioxidant, and anticancer properties, CS-CuO NPs are proving to be a versatile agent in healthcare with the potential for a wide range of medical applications and therapeutic advances (Alturki 2022; Alvi *et al.* 2024; Sarfraz *et al.* 2023)

Chlorophyll, the green pigment found in plants and algae, plays a crucial part in photosynthesis, absorbing light energy for converting carbon dioxide and water into glucose and oxygen. Its bright color depicts the essence of biological life processes (Agathokleous *et al.* 2020; Ong *et al.* 2024; Zhang *et al.* 2024). Combining chlorophyll with nanoparticles improves drug delivery, imaging, and antibacterial efficiency, making it useful in biomedicine and food preservation. Mixing chlorophyll with CS improves its stability, effectiveness, and antioxidant action. CS is a carrier, preventing chlorophyll decomposition and increasing absorption, enhancing its potential health benefits (Alkahtani *et al.* 2020; Balusamy *et al.* 2022; Hanafy *et al.* 2021; Pucci *et al.* 2021). Mixing chlorophyll with CuO NPs enhances its antimicrobial properties due to the synergistic effect between chlorophyll and Cu ions. This mixture can successfully suppress microbial development, which may help with several biomedical and food preservation applications (Alves Batista de Souza *et al.* 2024; Gautam *et al.* 2016; Liu *et al.* 2022; Perreault *et al.* 2010; Sharma *et al.* 2019). When ZnO and chlorophyll merge, ZnO's antioxidant and UV-blocking properties are strengthened. This combination offers a strong defense against damaging UV rays and oxidative stress, making it a promising candidate for use in sunscreen and skin care products (Adil *et al.* 2022; Chen *et al.* 2023; Haghighatzadeh 2021; Siddiqui *et al.* 2019).

A convincing aspect of the current investigation is the effect of chlorophyll-enriched CuO-CS-ZnO NPs on *X. axonopodis pv. Punicae* bacterial strain. *Xanthomonas axonopodis pv. punicae* primarily attacks pomegranate trees, leading to pomegranate bacterial blight. It can also infect other plants of the same family, including several species of the Punica genus and certain ornamental plants from the Lythraceae family. The study also investigates the implications of *Alternaria solani* growth, which is the causal agent of diseases affecting tomatoes, eggplants, and other vegetable crops. Furthermore, the study investigates the effect of CuO-CS-ZnO-Chlo NPs coatings on tomato preservation during subsequent storage. Furthermore, this study focuses on the optical, thermal, and morphological aspects of CuO-CS-ZnO-Chlo NPs.

2. Materials and methods

2.1 Material needed

Chitosan powder, acetic acid (CH_3COOH, 99.5%), hydrogen peroxide (H_2O_2, 98%), sodium hydroxide (NaOH, 97%), ammonia solution (NH_3), ethanol (C_2H_5OH), copper acetate monohydrate (Cu $(CH_3COO)_2{\cdot}H_2O$, 99%), zinc acetate dihydrate (Zn $(CH_3COO)_2{\cdot}2H_2O$, 99%). Chemicals were purchased from Sigma-Aldrich. Additionally, spinach leaves were used for chlorophyll extraction.

2.2 Extraction of Chlorophyll from Spinach Leaves

Spinach leaves were crushed and mixed with ethanol. Later, the solution was filtered to get the chlorophyll.

2.3 Preparation of $CuO_{0.35}CS_{0.3}ZnO_{0.35}$ -Chlorophyll NPs

A 1.0% (w/v) CS solution was dissolved in 1% (v/v) acetic acid. 17.5 mL of 0.1 M Cu $(CH_3COO)_2{\cdot}H_2O$, 99% and 17.5 mL of 0.1 M Zn $(CH_3COO)_2{\cdot}2H_2O$ were added to 15 mL of CS solution. That solution was combined with the chlorophyll solution at a 1:1 ratio (v/v). To reach a pH of 7-10, the combinations were adjusted with 0.1 M NaOH and thoroughly mixed for 4 hours at 100 °C. Finally, 3 hours of drying at 120 °C and 4 hours of annealing at 450 °C.

2.4 Characterization and Instrumentation

The crystal structure of CuO-Cs-ZnO-Chlo NPs was evaluated by XRD. Diffraction patterns from 10° to 55° were obtained at 50 kV and 40 mA. Cu-Kα radiation (BTX-646) was used for the XRD evaluation. By utilizing the Shimadzu-1800 UV-Vis spectrometer, the absorbance of the produced NPs was measured between 280 and 800 nm. The Shimadzu FTIR-8400 model was used to perform FTIR spectroscopy across a 400–4000 cm^{-1} range. SEM (SU-1500) was used to analyze the structure of NPs. Utilizing TGA (STA 449 F3 version), the thermal stability of CuO-CS-ZnO-Chlo NPs was evaluated. This was done in air-environment at temperatures ranging from 60-540 °C, with a heating rate of 10 °C/min and a flow rate of 50 mL/min. The antibacterial assessments focused on the Gram-negative bacterium *X. axanopodis pv punicea*. The antibacterial efficacy of the material was evaluated using the agar plate method (MIR-154-PE). Additionally, the agar well diffusion technique was used to study antifungal activities of the synthesized NPs on *Alternaria solani*. Tomatoes went through a series of steps to access food protection. They were first cleaned and sanitized with colloidal silver solution, then drained to remove any remaining water. The tomatoes were then treated by immersing them in water, letting them drain and air dry at room temperature. An Agrocolor colorimeter was used to measure changes in the surface color of the tomatoes. To understand the red component (R) and green component (G) using the CIE Lab scale [L* (lightness), a* (red-green color component)], a white teflon plate was calibrated. The texture properties of the tomatoes, including hardness and compression load, were assessed using a Brookfield CT3 texture meter in piercing and compression tests. HI 208 P.H. meter was used to determine the tomatoes' pH. Furthermore, a 503 nm wavelength was used to generate a lycopene calibration curve using a Genesys 10S UV-Vis spectrophotometer.

3. Results and discussion

3.1 Structural analysis

XRD analysis is critical for understanding the structure of the synthesized material and ensuring that the nanocomposites are successfully created. The XRD pattern in Figure 1(a) shows a detailed structural composition with distinct crystal peaks and noticeable amorphous characteristics. The provided sample reveals trichotomous structures. It highlights the intricate essence of CS and illustrates its trichotomous character by embodying amorphous, crystalline, and transitional properties. The inset of Figure 1(a) distinctly illustrates XRD peaks located at 12.5°, 16.6°, and 17.8°, corresponding to the (101), (002), and (121) crystallographic planes, respectively. These crystallographic planes are characteristic of CS, with an orthorhombic structure and lattice parameters a = 8.2, b = 16.4, and c = 10.3 in concordance with the JCPDS card: 00-039-1894. The three discernible XRD peaks at 37°, 40°, and 42.5° are related to ZnO, which have been allocated to the (101), (103), and (112) crystallographic planes, respectively. These results confirm ZnO's hexagonal wurtzite structure, consistent with previous investigations (Zaman *et al.* 2022). The crystallographic planes (200) and (111) of CuO are represented by prominent XRD peaks at 41.5° and 45° respectively. These findings support previous studies that found that CuO has a cubic crystal structure (Magesh *et al.* 2018; Thakar *et al.* 2022). The results are also consistent with the information on JCPDS card 01-078-2076. The detection of three distinct phases in the XRD pattern signifies the accomplished synthesis of CuO-CS-ZnO-Chlo NPs. Utilizing the Scherrer formula, the crystallite size of the NPs was calculated (Collins *et al.* 2012; Kawsar *et al.* 2024). The average crystallite size of ~10.7 nm was found. SEM images of the NPs are depicted in figure 1(c&d). At a given magnification, it is clear that the particles are not separated. Particle clustering exhibiting clear agglomeration and further showing the existence of voids within the material. Figure 1(b) shows the grain size distribution of the prepared NPs. These results are consistent with earlier research (Alharbi *et al.* 2023; Benazir *et al.* 2011).

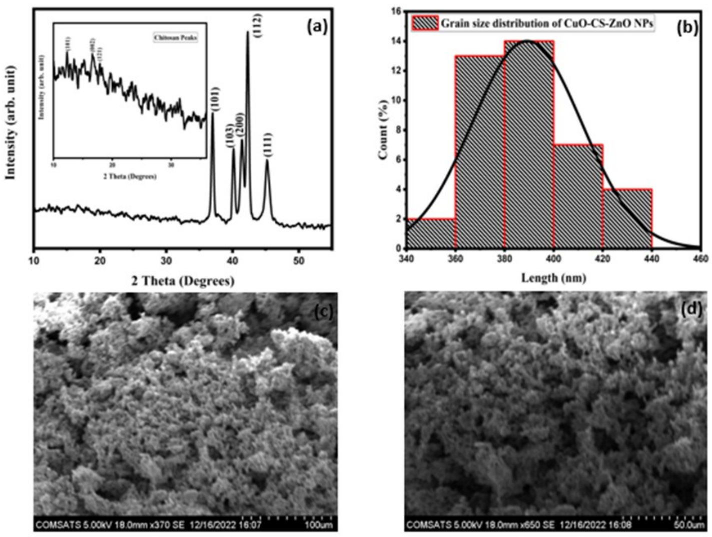

Figure 1. XRD pattern (a) size distribution (b) SEM image at 100 µm (c), and SEM image at 50 µm (d) of CuO-CS-ZnO-Chlo NPs

3.2 Optical analysis

Figure 2(a) shows the UV-Vis absorption spectrum of CuO-CS-ZnO-Chlo NPs. Sample absorption ceases around 450 nm. On zooming in the initial part of the absorption spectrum, three different absorption bands can be seen. Initial strong absorption could be associated with the absorption of glass material used as the substrate for NPs. Additional absorption bands in the range between 283-300 nm are associated with CuO-CS-ZnO-Chlo NPs. (Alshammari 2022; Arab-Bafrani *et al.* 2021; Gupta *et al.* 2015; Keabadile *et al.* 2020; Khazaal *et al.* 2020; Muiz *et al.* 2022; Nandiyanto *et al.* 2019; Rilda *et al.* 2022). FTIR spectrum of CuO-CS-ZnO-Chlo NPs is depicted in figure 2 (b). Functional groups associated with the formation of NPs are observed in FTIR. The transmittance peak at 500 cm^{-1} indicates the presence of metal ions, Cu or Zn, that are linked to the oxygen atoms. The presence of hydroxyl (-OH) groups is indicated at 1380 cm^{-1}. This is compatible with the hydrophilic nature of metal oxides and the -OH groups in the chlorophyll molecule. The stretching vibrations of carbon-carbon double bonds (C=C) correspond to the band around 1650 cm^{-1}. This signal shows the presence of unsaturated organic molecules, possibly chlorophyll with conjugated double bonds. The intense peak at 2920 cm^{-1} corresponds to the stretching vibrations of carbon-hydrogen (C-H) bonds. This is typical of organic compounds and further suggests the presence of CS and possibly other organic components. The presence of amino (-NH) groups is shown by the broad and strong band around 3460 cm^{-1}. This also suggests the presence of CS that includes amino groups (Asgari-Targhi *et al.* 2021; Kayani *et al.* 2015; Magesh *et al.* 2018; Rathore *et al.* 2020; Sankar *et al.* 2014; Seydi *et al.* 2019; Zhang *et al.* 2008).

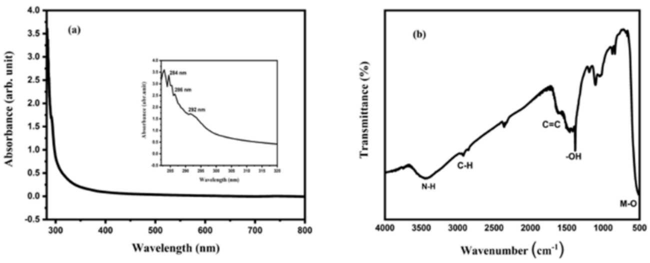

Figure 2. UV-vis absorption curve. The inset shows the magnified curve (a) and FTIR pattern (b) of CuO-CS-ZnO-Chlo NPs with the inclusion of chlorophyll

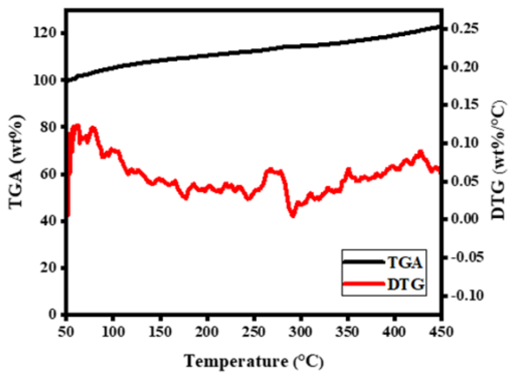

Figure 3. TGA-DTG patterns of CuO-CS-ZnO-Chlo NPs

3.3 Thermal evaluation

Figure 3 shows how the TGA-DTG results profoundly reveal the temperature-dependent effects of CuO-CS-ZnO-Chlo NPs. These NPs show initial weight gain that an oxidation process might have caused. Later, with small fluctuations, the weight of the materials stays constant throughout the measured temperature range. The material's enhanced thermal stability results from the synergistic co-doping of CS with ZnO and CuO. Minimal weight loss and modest changes imply thermal stability, the absence of volatile components, or effective decomposition resistance. Research shows strong bonding and high-purity materials exhibit such patterns, indicating their suitability for high-temperature applications. (Jayaramudu *et al.* 2019; Karpuraranjith and Thambidurai 2017; Kumar *et al.* 2019; Ltaief *et al.* 2021; Valiollahi *et al.* 2019; Wang *et al.* 2012).

3.4 Tomato preservation using CuO-CS-ZnO NPs

Tomatoes' color, which is important for market acceptance, varies as they ripen because of variations in their lycopene and chlorophyll contents. This change is quantified by parameters like L* and a*, where L* stands for lightness and a* for the ripeness indicator—the move from green to red. CuO-CS-ZnO-Chlo NPs-treated tomatoes postpone ripening-associated color changes by maintaining constant L* levels (33-41) and less variable a* values (31-44) over the course of a 15-day testing session. CuO-CS-ZnO-Chlo NPs prevent softening by preserving cell wall structure and turgor pressure, which also helps to retain firmness. Taste is impacted by the pH rising from 3.5 to 4 while being stored. Tomatoes that have been treated exhibit longer color retention and a reduced lycopene concentration over time. Through the modulation of membrane features during refrigeration at 12–16 °C, NPs have a good impact on quality parameters, contributing to practical preservation and increasing shelf life (Anthon and Barrett 2012; Belović *et al.* 2015; Del Real-López *et al*.; Esserti *et al.* 2024; Gopinath *et al.* 2024; Murtaza, Rizwan, *et al.* 2024; Murtaza, Usman, Iqbal, Tahir, *et al.* 2024; Pinheiro *et al.* 2013; Saei *et al.* 2011).

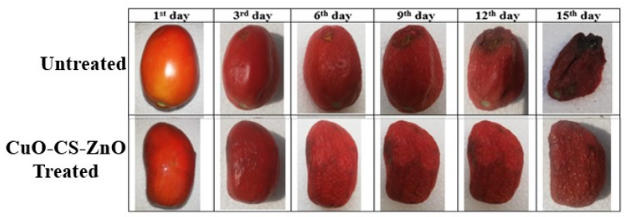

Figure 4. Preservation of tomatoes by utilizing CuO-CS-ZnO-Chlo NPs

3.5 Antibacterial effects

Figures 5 (a, b, c & d) display how well CuO-CS-ZnO-Chlo NPs stopped the growth of harmful bacteria. When more NPs were used, they worked better against *X. axanopodis pv punicea* bacteria after 24 and 48 hours**.** These NPs showed significant antibacterial effects and hence could be used to cure seeds and leaves suffering from bacterial diseases. In previous investigations, these NPs were found to exhibit substantial antibacterial activities against a wide range of diseases, demonstrating their efficiency in limiting microbial development. The NPs have demonstrated exceptional stability and biocompatibility, making them appropriate for a variety of applications, including medical and agricultural industries. After 24 hours the inhibition zone was 26 mm for 25%, 28 mm for 50%, and 29 mm for 75% of NPs. Later, the same observation was done after 48 our and the results were: 30 mm for 25%, 33 mm for 50%, and 35 mm for 75% of NPs in addition, chlorophyll also played a possible role in the enhancement of antibacterial effects. The treated seeds and plants exhibited reduced infection symptoms, highlighting the importance of these NPs in protecting against harmful bacteria, and contributing to healthier crops (Sibiya and Sumbwanyambe 2019). The interaction between nano-Zn and nano-Cu and bacteria is initiated by Cu and Zn adhesion to the cell membrane. This results in morphological changes, membrane depolarization, and intracellular leakage, which ultimately leads to cell death (Fayaz *et al.* 2010; Roy *et al.* 2019).

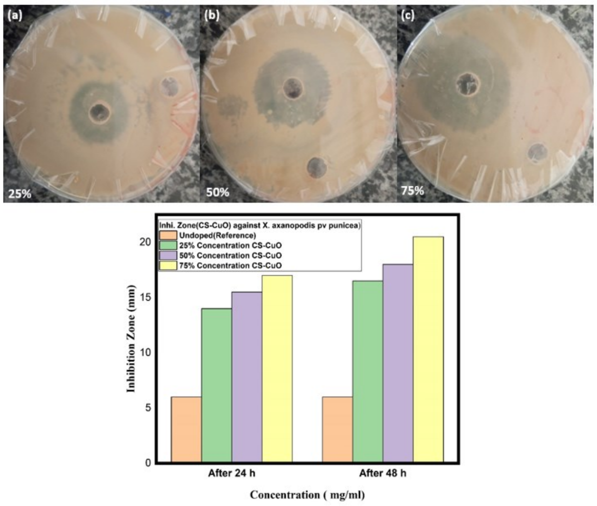

Figure 5. Antibacterial activity of CuO-CS-ZnO-Chlo NPs with the inclusion of chlorophyll against X. axanopodis pv punicea. Discs showed (a) 25% (b) 50% (c) 75% of NPs concentrations and (d) a bar chart depicting the inhibition zone after 24 and 48 hours at three different concentrations

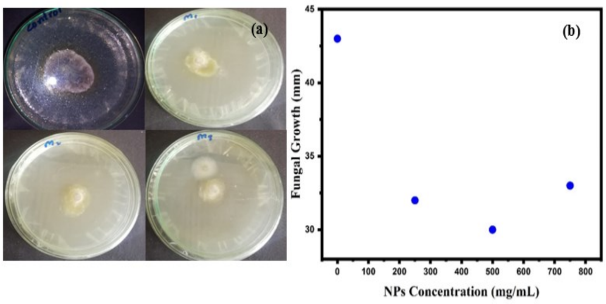

Figure 6. (a) Discs used for determining antifungal activity at different NPs concentration (b) antifungal activity of CuO-CS-ZnO-Chlo NPs against Alternaria solani

3.6 Antifungal effects

CuO-CS-ZnO-Chlo NPs were used in this study as a biocontrol agent against the *Alternaria solani* fungus. Significant antifungal efficacy was demonstrated by agar well diffusion analysis, shown in figure 6 (a), which showed a discernible decrease in *Alternaria solani* growth with increasing CuO-CS-ZnO-Chlo NPs concentrations. The computed observed growth rates at 0 mg/mL, 250 mg/mL, 500 mg/mL, and 750 mg/mL concentrations of CuO-CS-ZnO-Chlo NPs are shown in figure 6 (b). The corresponding measurements are 43 mm, 32 mm, 30 mm, and 33 mm. This demonstrates the promising effect of CuO-CS-ZnO-Chlo NPs on fighting the targeted fungus, especially when combined with chlorophyll. These NPs were very effective in inhibiting the fungus, even at low concentrations and beneficial for the health of plants (Mohamed A. Mosa and Sozan E. El-Abeid 2023; M. A. Mosa and S. E. El-Abeid 2023)

4. **Conclusions**

CuO-CS-ZnO NPs containing chlorophyll were synthesized by utilizing the sol-gel method. Structural and optical analysis confirmed the effective synthesis of NPs with an average crystallite size of 10.7 nm. Thermal analysis revealed the stability of the prepared CuO-CS-ZnO-Chlo NPs. CuO-CS-ZnO-Chlo NPs showed good antibacterial activity against *X. axanopodis pv punicea* bacteria and modest antifungal properties for *Alternaria solani*. Elevated NP concentrations boosted both antibacterial and antifungal activities. The use of these NPs has the potential to improve preservation quality, particularly by extending the shelf life of tomatoes.

Declaration of competing interest

The authors declare that they have no competing financial interests or personal relationships that could have appeared to influence the work reported in this paper.

Acknowledgments

We extend our sincere gratitude to Dr. Muhammad Farooq Qayyum and Dr. Muhammad Sajid from the Department of Soil Science, Bahauddin Zakariya University, for their invaluable assistance with X-ray crystallography (XRD). The authors also extend their appreciation to the Researchers supporting project number (RSP2024R470), King Saud University, Riyadh, Saudi Arabia.

References

Abdelrazek E.M., Elzayat A.M., Elbana A.A. and Awad W.M. (2023). Physical properties of copper oxide nano-composite incorporated PVP/chitosan blend matrix by casting method. *Polymer Bulletin*, 1–13.

Abdolsattari P., Rezazadeh-Bari M. and Pirsa S. (2022). Smart film based on polylactic acid, modified with polyaniline/ZnO/CuO: Investigation of physicochemical properties and its use of intelligent packaging of orange juice. *Food and Bioprocess Technology*, **15**(12), 2803–2825.

Adil M., Bashir S., Bashir S., Aslam Z., Ahmad N., Younas T. and Elshikh M.S. (2022). Zinc oxide nanoparticles improved chlorophyll contents, physical parameters, and wheat yield under salt stress. *Frontiers in plant science*, **13**, 932861.

Agathokleous E., Feng Z. and Peñuelas J. (2020). Chlorophyll hormesis: are chlorophylls major components of stress biology in higher plants? *Science of The Total Environment*, **726**, 138637.

Ahila K.G., Vasanthy M. and Thamaraiselvi C. (2018). Green synthesis of magnetic iron nanoparticle using Moringa oleifera Lam seeds and its application in textile effluent treatment.

Alharbi F.N., Abaker Z.M. and Makawi S.Z.A. (2023). Phytochemical substances—Mediated synthesis of zinc oxide nanoparticles (ZnO NPS). *Inorganics*, **11**(8), 328.

Alkahtani M.D.F., Attia K.A., Hafez Y.M., Khan N., Eid A.M., Ali M.A.M. and Abdelaal K.A.A. (2020). Chlorophyll fluorescence parameters and antioxidant defense system can display salt tolerance of salt acclimated sweet pepper plants treated with chitosan and plant growth promoting rhizobacteria. *Agronomy*, **10**(8), 1180.

Almaieli L.M.A., Khalaf M.M., Gouda M., Elmushyakhi A., Abou Taleb M.F. and Abd El-Lateef H.M. (2022). Fabrication of Bio-Based Film Comprising Metal Oxide Nanoparticles Loaded Chitosan for Wound Dressing Applications. *Polymers*, **15**(1), 211.

Alshammari F.H. (2022). Physical characterization and dielectric properties of chitosan incorporated by zinc oxide and graphene oxide nanoparticles prepared via laser ablation route. *Journal of Materials Research and Technology*, **20**, 740–747.

Alturki A.M. (2022). Facile synthesis route for chitosan nanoparticles doped with various concentrations of the biosynthesized copper oxide nanoparticles: Electrical conductivity and antibacterial properties. *Journal of Molecular Structure*, **1263**, 133108.

Alves Batista de Souza A., Souza E.R.d., Paraizo T.d. S. and Nascimento C.W.A.d. (2024). Mineral composition and chlorophyll fluorescence in cowpea plants amended with bulk and nanoparticles of Zn and Cu oxides. *Journal of Plant Nutrition*, 1–15.

Alvi A., Alqassim S., Khan N.A., Khatoon B., Akbar N., Kawish M. and Alfahemi H. (2024). Antibacterial effects of quercetagetin are significantly enhanced upon conjugation with chitosan engineered copper oxide nanoparticles. *BioMetals*, **37**(1), 171–184.

Anthon G.E. and Barrett D.M. (2012). Pectin methylesterase activity and other factors affecting pH and titratable acidity in processing tomatoes. *Food Chemistry*, **13*2***(2), 915–920.

Arab-Bafrani Z., Zabihi E., Jafari S.M., Khoshbin-Khoshnazar A., Mousavi E., Khalili M. and Babaei A. (2021). Enhanced radiotherapy efficacy of breast cancer multi cellular tumor spheroids through in-situ fabricated chitosan-zinc oxide bio-nanocomposites as radio-sensitizing agents. *International Journal of Pharmaceutics*, **605**, 120828.

Asgari-Targhi G., Iranbakhsh A., Ardebili Z.O. and Tooski A.H. (2021). Synthesis and characterization of chitosan encapsulated zinc oxide (ZnO) nanocomposite and its biological assessment in pepper (Capsicum annuum) as an elicitor for in vitro tissue culture applications. *International journal of biological macromolecules*, **189**, 170–182.

Balusamy S.R., Rahimi S., Sukweenadhi J., Sunderraj S., Shanmugam R., Thangavelu L. and Perumalsamy H. (2022). Chitosan, chitosan nanoparticles and modified chitosan biomaterials, a potential tool to combat salinity stress in plants. *Carbohydrate Polymers*, **284**, 119189.

Baroudi A., García-Payo C. and Khayet M. (2023). Chitosan-Based Composite Membranes with Different Biocompatible Metal Oxide Nanoparticles: Physicochemical Properties and Drug-Release Study. *Polymers*, **15**(13), 2804.

Belović M., Kevrešan Ž., Pestorić M. and Mastilović J. (2015). The influence of hot air treatment and UV irradiation on the quality of two tomato varieties after storage. *Food Packaging and Shelf Life*, **5**, 63–67.

Benazir J.F., Suganthi R., Anjana Hari A.H., Kumar V.R., Aswathi M.P., Niraimathi G. and Santhi R. (2011). Bio utilization of agroindustrial waste in solid state fermentation by Aspergillus niger for the production of protease.

Benettayeb A., Seihoub F.Z., Pal P., Ghosh S., Usman M., Chia C. H. and Sillanpää M. (2023). Chitosan nanoparticles as potential nano-sorbent for removal of toxic environmental pollutants. *Nanomaterials*, **13**(3), 447.

Bolaina-Lorenzo E., Puente-Urbina B.A., Espinosa-Neira R., Ledezma A., Rodríguez-Fernández O. and Betancourt-Galindo R. (2022). A simple method to improve antibacterial properties in commercial face masks via incorporation of ZnO and CuO nanoparticles through chitosan matrix. *Materials Chemistry and Physics*, **287**, 126299.

Boshkova N., Kamburova K., Radeva T., Simeonova S., Grozev N. and Boshkov N. (2023). Hybrid Zinc Coatings with Chitosan/Alginate Encapsulated CuO-Nanoparticles for Anticorrosion and Antifouling Protection of Mild Steel. *Coatings*, **13**(5), 895.

Chen F., Li Y., Zia-ur-Rehman M., Hussain S.M., Qayyum M.F., Rizwan M. and Ali S. (2023). Combined effects of zinc oxide nanoparticles and melatonin on wheat growth, chlorophyll contents, cadmium (Cd) and zinc uptake under Cd stress. *Science of The Total Environment*, **864**, 161061.

Chen L., Li X., Chen J., Lin R., Mai Y., Lin Y. and Wang J. (2024). Formulation with zinc acetate enhances curcumin's inherent and photodynamic antimicrobial effects for food preservation. *Food Control*, **157**, 110200.

Collins D., Luxton T., Kumar N., Shah S., Walker V.K. and Shah, V. (2012). Assessing the impact of copper and zinc oxide nanoparticles on soil: a field study.

Del Real-López A., González-Reza R.M., Zambrano-Zaragoza M.L., Miranda-Linares, V. and Escamilla-Rendón P. (2016). Solid lipid nanoparticles based edible coating for saladette tomato preservation.

Dizaj S.M. (2015). Calcium carbonate nanoparticles; potential in bone and tooth disorders (Pharmaceutical Sciences **20**) (Iran. In: Tuoms Press) p.

Espitia P.J.P., Soares N.d.F.F., Coimbra J.S.d.R., de Andrade N.J., Cruz R.S. and Medeiros E.A.A. (2012). Zinc oxide nanoparticles: synthesis, antimicrobial activity and food packaging applications. *Food and Bioprocess Technology*, **5**, 1447–1464.

Esserti S., Billah R.E.K., Venisse J.-S., Smaili A., Dich J., Es-sahm I. and Choukri R. (2024). Chitosan embedded with ZnO nanoparticles and hydroxyapatite: synthesis, antiphytopathogenic activity and effect on tomato grown under high density. *Scientia Horticulturae*, **326**, 112778.

Fan X., Zhu J., Duan C., Sun P., Chen Q., Kong B. and Wang H. (2024). Oregano essential oil encapsulated in zein-pectin-chitosan nanoparticles to improve the storage quality of Harbin red sausage. *International journal of biological macromolecules*, 131322.

Fayaz A.M., Balaji K., Girilal M., Yadav R., Kalaichelvan P.T. and Venketesan R. (2010). Biogenic synthesis of silver nanoparticles and their synergistic effect with antibiotics: a study against gram-positive and gram-negative bacteria. *Nanomedicine: Nanotechnology, Biology and Medicine*, **6**(1), 103–109.

Fonseca D.R., Alves P.M., Neto E., Custódio B., Guimarães S., Moura D. and Teixeira C. (2024). One-Pot Microfluidics to

Engineer Chitosan Nanoparticles Conjugated with Antimicrobial Peptides Using “Photoclick” Chemistry: Validation Using the Gastric Bacterium Helicobacter pylori. *ACS applied materials and interfaces*.

Gautam S., Misra P., Shukla P.K. and Ramteke P.W. (2016). Effect of copper oxide nanoparticle on the germination, growth and chlorophyll in soybean (Glycine max L.). *Vegetos*, **29**, 157–160.

Ghosh C., Bera D. and Roy L. (2019). Role of nanomaterials in food preservation. *Microbial Nanobionics: Volume 2, Basic Research and Applications*, 181–211.

Gopinath K., Sathishkumar G. and Xu L. (2024). An Overview of the Copper Oxide Nanofillers Integrated in Food Packaging Systems. *Coatings*, **14**(1), 81.

Govindasamy G.A., Smn Mydin R.B., Gadaime N.K.R. and Sreekantan S. (2023). Phytochemicals, biodegradation, cytocompatibility and wound healing profiles of chitosan film embedded green synthesized antibacterial ZnO/CuO nanocomposite. *Journal of Polymers and the Environment*, **31**(10), 4393–4409.

Gunaki M.N., Masti S.P., D'Souza O.J., Eelager M.P., Kurabetta L.K., Chougale R.B. and Kumar S.K.P. (2024). Fabrication of CuO nanoparticles embedded novel chitosan/hydroxypropyl cellulose bio-nanocomposites for active packaging of jamun fruit. *Food Hydrocolloids*, 109937.

Gupta S., Dubey S.K. and Prakash R. (2015). Genosensor based on a nanostructured, platinum-modified glassy carbon electrode for Listeria detection. *Analytical Methods*, **7**(6), 2616–2622.

Haghighatzadeh A. (2021). Visible-light-active chlorophyll/flavonoid-sensitized ZnO nanoparticles: preparation and optical and photocatalytic studies. *Journal of the Australian Ceramic Society*, **57**(1), 137–147.

Hajipour M.J., Fromm K.M., Ashkarran A.A., de Aberasturi D.J., de Larramendi I.R., Rojo T. and Mahmoudi M. (2012). Antibacterial properties of nanoparticles. *Trends in biotechnology*, **30**(10), 499–511.

Hanafy N.A.N., Leporatti S. and El-Kemary M.A. (2021). Extraction of chlorophyll and carotenoids loaded into chitosan as potential targeted therapy and bio imaging agents for breast carcinoma. *International journal of biological macromolecules*, **182**, 1150–1160.

Hermanto D., Ismillayli N., Fatwa D.H., Zuryati U.K., Muliasari H., Wirawan R. and Suprapto S. (2024). Bio-mediated electrochemically synthesis of silver nanoparticles using green tea (Camellia sinensis) leaves extract and their antibacterial activity. *South African Journal of Chemical Engineering*, **47**(1), 136–141.

Ibrahim N.A., Ameen H.A. and Eid B.M. (2024). Green synthesized chitosan and ZnO nanoparticles for sustainable use in multifunctionalization of cellulosic fabrics. *Polymer Bulletin*, **81**(4), 3621–3640.

Jalal R.R., Ways T.M.M., Elella M.H.A., Hassan D.A. and Khutoryanskiy V.V. (2023). Preparation of mucoadhesive methacrylated chitosan nanoparticles for delivery of ciprofloxacin. *International journal of biological macromolecules*, **242**, 124980.

Jayaramudu T., Varaprasad K., Pyarasani R.D., Reddy K.K., Kumar K.D., Akbari-Fakhrabadi A. and Amalraj J. (2019). Chitosan capped copper oxide/copper nanoparticles encapsulated microbial resistant nanocomposite films. *International journal of biological macromolecules*, **128**, 499–508. https://doi.org/https://doi.org/10.1016/j.ijbiomac.2019.01.145

Jha R. and Mayanovic R.A. (2023). A review of the preparation, characterization, and applications of chitosan nanoparticles in nanomedicine. *Nanomaterials*, **13**(8), 1302.

Jiang R., Zhu H.-Y., Zang X., Fu Y.-Q., Jiang S.-T., Li J.-B. and Wang Q. (2023). A review on chitosan/metal oxide nanocomposites for applications in environmental remediation. *International journal of biological macromolecules*, 127887.

Karpuraranjith M. and Thambidurai S. (2017). Chitosan/zinc oxide-polyvinylpyrrolidone (CS/ZnO-PVP) nanocomposite for better thermal and antibacterial activity. *International journal of biological macromolecules*, **104**, 1753–1761. https://doi.org/https://doi.org/10.1016/j.ijbiomac.2017.02.079

Kawsar M., Hossain M.S., Bahadur N.M. and Ahmed S. (2024). Synthesis of nano-crystallite hydroxyapatites in different media and a comparative study for estimation of crystallite size using Scherrer method, Halder-Wagner method size-strain plot, and Williamson-Hall model. *Heliyon*, **10**(3).

Kayani Z.N., Umer M., Riaz S. and Naseem S. (2015). Characterization of copper oxide nanoparticles fabricated by the sol–gel method. *Journal of Electronic Materials*, **44**, 3704–3709.

Keabadile O.P., Aremu A.O., Elugoke S.E. and Fayemi O.E. (2020). Green and traditional synthesis of copper oxide nanoparticles—comparative study. *Nanomaterials*, **10**(12), 2502.

Khazaal F.A., Kadhim M.M., Husseein H.F., Abbas Z.M., Shamzah M., Khudhair I.A. and Saieed H.S. (2020). Electronic transfers and (nlo) properties predicted by ab initio methods with prove experimentally. *NeuroQuantology*, **18**(1), 46.

Khurshid Z., Zafar M., Qasim S., Shahab S., Naseem M. and AbuReqaiba A. (2015). Advances in nanotechnology for restorative dentistry. *Materials*, **8**(2), 717–731.

Kim I., Viswanathan K., Kasi G., Thanakkasaranee S., Sadeghi K. and Seo J. (2022). ZnO nanostructures in active antibacterial food packaging: preparation methods, antimicrobial mechanisms, safety issues, future prospects, and challenges. *Food Reviews International*, **38**(4), 537–565.

Kou S.G., Peters L.M. and Mucalo M.R. (2021). Chitosan: A review of sources and preparation methods. *International journal of biological macromolecules*, **169**, 85–94.

Kumar S., Krishnakumar B., Sobral A.J.F.N. and Koh J. (2019). Bio-based (chitosan/PVA/ZnO) nanocomposites film: Thermally stable and photoluminescence material for removal of organic dye. *Carbohydrate Polymers*, **205**, 559–564. https://doi.org/https://doi.org/10.1016/j.carbpol.2018.10.108

Liu Z., Guo S., Fang X., Shao X. and Zhao Z. (2022). Antibacterial and plant growth-promoting properties of novel Fe 3 O 4/Cu/CuO magnetic nanoparticles. *RSC advances*, **12**(31), 19856–19867.

Ltaief S., Jabli M. and Ben Abdessalem S. (2021). Immobilization of copper oxide nanoparticles onto chitosan biopolymer: Application to the oxidative degradation of Naphthol blue black. *Carbohydrate Polymers*, **261**, 117908. https://doi.org/10.1016/j.carbpol.2021.117908

Magesh G., Bhoopathi G., Nithya N., Arun A.P. and Kumar E.R. (2018). Tuning effect of polysaccharide chitosan on structural, morphological, optical and photoluminescence properties of ZnO nanoparticles. *Superlattices and Microstructures*, **117**, 36–45.

Matyjasik W., Długosz O., Lis K. and Banach M. (2022). Nanohybrids of oxides nanoparticles-chitosan and their antimicrobial properties. *Nanotechnology*, **33**(43), 435701.

Mosa M.A. and El-Abeid S.E. (2023). Chitosan-Loaded Copper Oxide Nanoparticles: A Promising Antifungal Nanocomposite against Fusarium Wilt Disease of Tomato Plants. *Sustainability*, **15**(19), 14295.

Mosa M.A. and El-Abeid S.E. (2023). Chitosan-Loaded Copper Oxide Nanoparticles: A Promising Antifungal Nanocomposite against Fusarium Wilt Disease of Tomato Plants. Sustainability, **15**, 14295. In.

Muiz L.J., Juwono A.L. and Krisnandi Y.K. (2022). A review: Silver–zinc oxide nanoparticles–organoclay-reinforced chitosan bionanocomposites for food packaging. *Open Chemistry*, **20**(1), 1155–1170.

Murtaza G., Ahmed Z., Usman M., Iqbal R., Zulfiqar F., Tariq A. and Ditta A. (2024). Physicochemical properties and performance of non-woody derived biochars for the sustainable removal of aquatic pollutants: A systematic review. *Chemosphere*, 142368.

Murtaza G., Rizwan M., Usman M., Hyder S., Akram M.I., Deeb M. and Ali M.R. (2024). Biochar enhances the growth and physiological characteristics of Medicago sativa, Amaranthus caudatus and Zea mays in saline soils. *BMC Plant Biology*, **24**(1), 304.

Murtaza G., Usman M., Iqbal J., Hyder S., Solangi F., Iqbal R. and Tariq W. (2024). Liming potential and characteristics of biochar produced from woody and non-woody biomass at different pyrolysis temperatures. *Scientific reports*, **14**(1), 11469.

Murtaza G., Usman M., Iqbal J., Tahir M.N., Elshikh M.S., Alkahtani J. and Gruda N.S. (2024). The impact of biochar addition on morpho-physiological characteristics, yield and water use efficiency of tomato plants under drought and salinity stress. *BMC Plant Biology*, **24**(1), 356.

Nandiyanto A.B.D., Oktiani R. and Ragadhita R. (2019). How to read and interpret FTIR spectroscope of organic material. *Indonesian Journal of Science and Technology*, **4**(1), 97–118.

Naseem T. and Durrani T. (2021). The role of some important metal oxide nanoparticles for wastewater and antibacterial applications: A review. *Environmental Chemistry and Ecotoxicology*, **3**, 59–75.

Neethidevan K., Ravichandran K., Ayyanar M., Kavitha P., Amalraj S., Mohan R. and Maheshwaran G. (2023). Wattakaka volubilis powered green synthesized CuO, NiO and ZnO nanoparticles for cost-effective biomedical applications. *Biomass Conversion and Biorefinery*, 1–15.

Nemr O.T., Abdel-wahab M.S., Hamza Z.S., Ahmed S.A., El-Bassuony A.A., Abdel-Gawad O.F. and Mohamed H.S. (2024). Investigating the Anticancer and Antioxidant Potentials of a Polymer-Grafted Sodium Alginate Composite Embedded with CuO and TiO2 Nanoparticles. *Journal of Polymers and the Environment*, 1–16.

Nizami M.Z.I., Xu V.W., Yin I.X., Yu O.Y. and Chu C.-H. (2021). Metal and metal oxide nanoparticles in caries prevention: A review. *Nanomaterials*, **11**(12), 3446.

Ong P., Jian J., Li X., Yin J. and Ma G. (2024). Visible and near-infrared spectroscopic determination of sugarcane chlorophyll content using a modified wavelength selection method for multivariate calibration. *Spectrochimica Acta Part A: Molecular and Biomolecular Spectroscopy*, **305**, 123477.

Parnia F., Yazdani J., Javaherzadeh V. and Dizaj S.M. (2017). Overview of nanoparticle coating of dental implants for enhanced osseointegration and antimicrobial purposes. *Journal of Pharmacy & Pharmaceutical Sciences*, **20**, 148–160.

Perreault F., Oukarroum A., Pirastru L., Sirois L., Matias W.G. and Popovic R. (2010). Evaluation of copper oxide nanoparticles toxicity using chlorophyll a fluorescence imaging in Lemna gibba. *Journal of Botany*.

Pinheiro J., Alegria C., Abreu M., Gonçalves E.M. and Silva C.L.M. (2013). Kinetics of changes in the physical quality parameters of fresh tomato fruits (Solanum lycopersicum, cv.'Zinac') during storage. *Journal of Food Engineering*, **114**(3), 338–345.

Poznanski P., Hameed A. and Orczyk W. (2023). Chitosan and chitosan nanoparticles: Parameters enhancing antifungal activity. *Molecules*, **28**(7), 2996.

Pucci C., Martinelli C., Degl'Innocenti A., Desii A., De Pasquale D. and Ciofani G. (2021). Light-activated biomedical applications of chlorophyll derivatives. *Macromolecular Bioscience*, **21**(9), 2100181.

Rajivgandhi G., Maruthupandy M. and Quero F. (2023). Investigation of Chitosan/Metal and Metal Oxide Nanocomposites as a New Strategy for Enhanced Anti-Biofilm Efficacy with Reduced Toxicity. In *Chitosan Nanocomposites: Bionanomechanical Applications* (349–375). Springer.

Rathore B.S., Chauhan N.P.S., Rawal M.K., Ameta S.C. and Ameta R. (2020). Chitosan–polyaniline–copper (II) oxide hybrid composite for the removal of methyl orange dye. *Polymer Bulletin*, **77**(9), 4833–4850.

Renzi D.F., de Almeida Campos L., Miranda E.H., Mainardes R.M., Abraham W.-R., Grigoletto D.F. and Khalil N.M. (2021). Nanoparticles as a tool for broadening antifungal activities. *Current Medicinal Chemistry*, **28**(9), 1841–1873.

Rilda Y., Ayuni P.V.P., Refinel R., Armaini A., Agustien A., Almurdi A. and Pardi H. (2022). ANTIBACTERIAL PROPERTIES AND UV-PROTECTION OF COTTON FABRIC USING NANOHYBRID MULTILAYER ZnO-SiO2/CHITOSAN AND DODECYLTRIETOXYSILANE (DTS). *Rasayan Journal of Chemistry*, **15**(1).

Roy A., Bulut O., Some S., Mandal A.K. and Yilmaz M.D. (2019). Green synthesis of silver nanoparticles: biomolecule-nanoparticle organizations targeting antimicrobial activity. *RSC advances*, **9**(5), 2673–2702.

Saei A., Tustin D.S., Zamani Z., Talaie A. and Hall A.J. (2011). Cropping effects on the loss of apple fruit firmness during storage: The relationship between texture retention and fruit dry matter concentration. *Scientia Horticulturae*, **130**(1), 256–265.

Said A., Abu-Elghait M., Atta H.M. and Salem S.S. (2024). Antibacterial activity of green synthesized silver nanoparticles using Lawsonia inermis against common pathogens from urinary tract infection. *Applied Biochemistry and Biotechnology*, **196**(1), 85–98.

Salama H.E. and Aziz M.S.A. (2023). Non-toxic chitosan-pyrazole adsorbent enriched with greenly synthesized zinc oxide nanoparticles for dye removal from wastewater. *International journal of biological macromolecules*, **241**, 124632.

Salas-Orozco M.F., Lorenzo-Leal A.C., de Alba Montero I., Marín N.P., Santana M.A.C. and Bach H. (2024). Mechanism of escape from the antibacterial activity of metal-based nanoparticles in clinically relevant bacteria: A systematic review. *Nanomedicine: Nanotechnology, Biology and Medicine*, **55**, 102715.

Saleem M.H., Ejaz U., Vithanage M., Bolan N. and Siddique K.H.M. (2024). Synthesis, characterization, and advanced sustainable applications of copper oxide nanoparticles: a review. *Clean Technologies and Environmental Policy*, 1–26.

Sankar R., Manikandan P., Malarvizhi V., Fathima T., Shivashangari K.S. and Ravikumar V. (2014). Green synthesis of colloidal copper oxide nanoparticles using Carica papaya and its application in photocatalytic dye degradation. *Spectrochimica Acta Part A: Molecular and Biomolecular Spectroscopy*, **121**, 746–750.

Sarfraz M.H., Zubair M., Ashraf A., Cruz J.N., Muzammil S. Hashem A. and Abd_Allah E.F. (2023). Comparative analysis of phyto-fabricated chitosan, copper oxide, and chitosan-based CuO nanoparticles: antibacterial potential against Acinetobacter baumannii isolates and anticancer activity against HepG2 cell lines. *Frontiers in Microbiology*, **14**, 1188743.

Serouti A., Eddine L.S., Meneceur S., Hasan G.G., Mohammed H.A., Salmi C. and Abdullah J.A.A. (2024). Biogenic ZnO/CuO/Fe2O3 Nanocomposite: A Groundbreaking Approach for Enhanced Degradation Capabilities and Reusability in Dye Removal Applications. *Arabian Journal for Science and Engineering*, **49**(1), 753–764.

Seydi N., Saneei S., Jalalvand A.R., Zangeneh M.M., Zangeneh A., Tahvilian R. and Pirabbasi E. (2019). Synthesis of titanium nanoparticles using Allium eriophyllum Boiss aqueous extract by green synthesis method and evaluation of their remedial properties. *Applied Organometallic Chemistry*, **33**(11), e5191.

Shankar V.S., Thulasiram R., Priyankka A.L., Nithyasree S. and Sharma A.A. (2024). Applications of Nanomaterials on a Food Packaging System—A Review. *Engineering Proceedings*, **61**(1), 4.

Sharma S., Uttam R., Sarika Bharti A. and Uttam K.N. (2019). Interaction of zinc oxide and copper oxide nanoparticles with chlorophyll: A fluorescence quenching study. *Analytical Letters*, **52**(10), 1539–1557.

Sibiya M. and Sumbwanyambe M. (2019). An algorithm for severity estimation of plant leaf diseases by the use of colour threshold image segmentation and fuzzy logic inference: a proposed algorithm to update a “leaf doctor” application. *AgriEngineering*, **1**(2), 15.

Siddiqui Z.A., Parveen A., Ahmad L. and Hashem A. (2019). Effects of graphene oxide and zinc oxide nanoparticles on growth, chlorophyll, carotenoids, proline contents and diseases of carrot. *Scientia Horticulturae*, **249**, 374–382.

Singh M., Singh S., Prasad S. and Gambhir I.S. (2008). Nanotechnology in medicine and antibacterial effect of silver nanoparticles. *Digest Journal of Nanomaterials and Biostructures*, **3**(3), 115–122.

Tang S. and Zheng J. (2018). Antibacterial activity of silver nanoparticles: structural effects. *Advanced Healthcare Materials*, **7**(13), 1701503.

Thakar M.A., Jha S.S., Phasinam K., Manne R., Qureshi Y. and Babu V.V.H. (2022). X ray diffraction (XRD) analysis and evaluation of antioxidant activity of copper oxide nanoparticles synthesized from leaf extract of Cissus vitiginea. *Materials Today: Proceedings*, **51**, 319–324.

Valiollahi M.H., Abbasian M. and Pakzad M. (2019). Synthesis and Characterization of Polyaniline-Polystyrene-Chitosan/Zinc Oxide Hybrid Nanocomposite. *Iranian Journal of Chemistry and Chemical Engineering*, **38**(5), 55–64.

Wang S., Huang X., He Y., Huang H., Wu Y., Hou L. and Huang B. (2012). Synthesis, growth mechanism and thermal stability of copper nanoparticles encapsulated by multi-layer graphene. *Carbon*, **50**(6), 2119–2125. https://doi.org/https://doi.org/10.1016/j.carbon.2011.12.063

Wu L., Lv S., Wei D., Zhang S., Zhang S., Li Z. and He T. (2023). Structure and properties of starch/chitosan food packaging film containing ultra-low dosage GO with barrier and antibacterial. *Food Hydrocolloids*, **137**, 108329.

Zaman H.G., Baloo L., Aziz F., Kutty S.R. and Ashraf A. (2022). COD adsorption and optimization from produced water using chitosan–ZnO nanocomposite. *Applied Nanoscience*, **12**(6), 1885-1898.

Zare M., Namratha K., Ilyas S., Sultana A., Hezam A., Surmeneva M.A. and Mathur S. (2022). Emerging trends for ZnO nanoparticles and their applications in food packaging. *ACS Food Science & Technology*, **2**(5), 763–781.

Zhang S., Tian J., Lu X., Tian Q., He S., Lin Y. and Mu X. (2024). Monitoring of chlorophyll content in local saltwort species Suaeda salsa under water and salt stress based on the PROSAIL-D model in coastal wetland. *Remote Sensing of Environment*, **306**, 114117.

Zhang T., Chen Y., Yu Q., Sun H., Chen K., Ye H. and Niu Q.J. (2023). Advanced Mg2+/Li+ separation nanofiltration membranes by introducing hydroxypropyltrimethyl ammonium chloride chitosan as a co-monomer. *Applied Surface Science*, **616**, 156434.

Zhang W., Sani M.A., Zhang Z., McClements D.J. and Jafari S.M. (2023). High performance biopolymeric packaging films containing zinc oxide nanoparticles for fresh food preservation: A review. *International journal of biological macromolecules*, **230**, 123188.

Zhang X., Wang G., Liu X., Wu J., Li M., Gu J. and Fang B. (2008). Different CuO nanostructures: synthesis, characterization, and applications for glucose sensors. *The Journal of Physical Chemistry C*, **112**(43), 16845–16849.